Power Electronics and Drives
Volume 4(39), 2019 DOI: 10.2478/pead-2019-0009

Power Electronics and Drives

An Investigation of Direct Torque Control and Hysteresis Current Vector Control for Motion Control Synchronous Reluctance Motor Applications

Research Article

Tibor Vajsz, László Számel, Árpád Handler

Department of Electric Power Engineering, Faculty of Electrical Engineering and Informatics, Budapest University of Technology and Economics, Budapest, Hungary

Received December 20, 2018; Accepted April 1, 2019

Abstract: Synchronous reluctance motor drives are one of the most attractive alternatives of permanent magnet synchronous motor drives and induction motor drives in the field of conventional industrial and household applications. This tendency is expected to be continued in the case of motion control applications as well. This article investigates two torque-control algorithms that are possible candidates for motion control synchronous reluctance motor applications. The examined torque-control algorithms are direct torque control (DTC) and hysteresis current vector control (HCVC).

Keywords: *synchronous reluctance motor • electric drive • direct torque control • current vector control • frequency converter • motion control • industrial drives*

1. Introduction

Nowadays, the alternatives for the widely used permanent magnet synchronous motor and induction motor drives are getting more and more attention. This is due to the fact that the former is still expensive and relatively sensitive to overheating and vibrations, while the latter has a limited power density and efficiency. The synchronous reluctance motor is one of the most promising alternatives of both motor drives due to its simple and robust construction, lack of permanent magnets, high power density and efficiency. Their price is competitive with that of the induction motor drives. These facts explain why the synchronous reluctance motor drives are getting more and more attention in many fields, especially within the field of conventional industrial and household applications (pumps, fans, compressors, etc.). This tendency is expected to be continued in the field of motion control applications as well.

However, the applied control algorithms have a fundamental effect on the quality features of a drive system as well. Therefore, in this article, an investigation is carried out for two torque-control algorithms that are possible candidates for motion control synchronous reluctance motor applications. The examined torque-control algorithms are direct torque control (DTC) and hysteresis current vector control (HCVC). Their main features are studied and compared in order to select the possible fields of application for the two methods.

* *E-mail: vajsz.tibor@vet.bme.hu, szamel.laszlo@vet.bme.hu, handler.arpad@gmail.com*

2. Basic Equations of Synchronous Reluctance Motor Drives

The synchronous reluctance motor is driven by the so-called reluctance torque. This torque becomes significant when the magnetic circuit of the motor is heavily asymmetric, which means that one part of the motor has a relatively low magnetic resistance (low-reluctance part), while the other part has a much higher magnetic resistance (high-reluctance part). In the case of the synchronous reluctance motor, the rotor structure is the source of the magnetic asymmetry and the torque is generated because the stator magnetic field tries to bring the rotor into alignment with itself. Therefore, it is reasonable to use a coordinate system that has its real axis fixed to the middle of the low-reluctance part of the rotor (this is called the d-axis), while the imaginary axis is fixed to the middle of the high-reluctance part of the rotor (this is called the q-axis). This coordinate system is called the d–q coordinate system.

In the d–q coordinate system, the relationships between the d- and the q-components of the stator voltage vector and the stator current vector are as follows (no damping cage is used):

$$\frac{v_d}{R} + \omega T_q i_q = i_d + T_d \frac{di_d}{dt} \tag{1}$$

$$\frac{v_q}{R} - \omega T_d i_d = i_q + T_q \frac{di_q}{dt} \tag{2}$$

where v_d and v_q are the d- and the q-components of the stator voltage vector, respectively; i_d and i_q are the d- and the q-components of the stator current vector, respectively; T_d and T_q are the d- and the q-axis electrical time constants, respectively; ω is the electrical speed of the rotor and R is the stator resistance.

According to Equations (1) and (2), there is a strong cross-coupling between the d- and the q-components of the stator voltage vector and the stator current vector. The T_d and the T_q electrical time constants can be defined as follows:

$$T_d = L_d / R \tag{3}$$

$$T_q = L_q / R \tag{4}$$

where L_d and L_q are the d- and the q-axis synchronous inductances, respectively. The following equations describe the stator flux vector (Fig. 1):

$$\psi_d = L_d i_d \tag{5}$$

$$\psi_q = L_q i_q, \tag{6}$$

where ψ_d and ψ_q are the d- and the q-components of the stator flux vector, respectively.

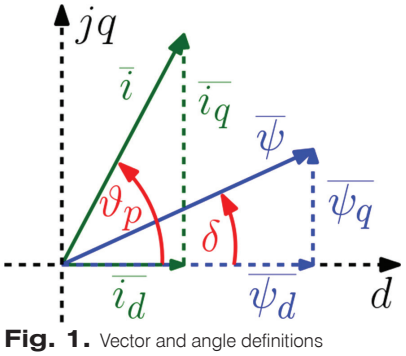

Fig. 1. Vector and angle definitions

The electromagnetic torque of the motor can be expressed as follows:

$$m = \frac{3}{4} p \left(L_d - L_q \right) i^2 \sin\left(2\vartheta_p \right) \tag{7}$$

where m is the electromagnetic torque, p is the number of pole pairs, i is the amplitude of the stator current vector and ϑ_p is the torque angle (the angle between the stator current vector and the d-axis; Fig. 1).

After a few equivalent transformations, Equation (7) can be further expressed as

$$m = \frac{3}{2} p \left(L_d - L_q \right) i_d i_q \tag{8}$$

Equations (7) and (8) suggest that the greater the $L_d - L_q$ inductance difference, the higher the electromagnetic torque that can be achieved with the same current. If $L_d = L_q$, no torque is produced. This corresponds to the fact that torque production is based on the magnetic asymmetry.

Equation (9) describes the motion law for rotating electric machines:

$$\omega_r = \frac{1}{J} \int_0^\tau \left(m(t) - m_1(t) \right) dt + \omega_{r0} \tag{9}$$

where ω_r is the mechanical angular velocity of the rotor, J is the moment of inertia for the total system reduced to the shaft of the motor, m_1 is the load torque reduced to the shaft of the motor and ω_{r0} is the initial mechanical angular velocity of the rotor.

In this model, the friction torque is taken into account as a part of the load torque. Iron losses of the stator are neglected. Equations (1), (2), (8) and (9) together form the differential equation system of the drive system. More details about the reluctance torque, synchronous reluctance motors and their basic equations can be read in Antonello et al. (2016), Bianchi et al. (2016), Guagnano et al. (2016), Hadla (2016), Hinkkanen et al. (2016), Ma et al. (2018), Nardo et al. (2018), Staudt et al. (2015) and Vajsz et al. (2017).

3. Direct Torque Control

In order to understand the basic principle of DTC, Equation (8) must be transformed into the following form:

$$m = \frac{3}{4} p \left(\frac{1}{L_q} - \frac{1}{L_d} \right) \psi^2 \sin\left(2\delta \right) \tag{10}$$

where δ is the load angle (the angle between the stator flux vector and the d-axis; Fig. 1) and ψ is the amplitude of the stator flux vector.

This means that the electromagnetic torque can be controlled by regulating the load angle and the amplitude of the stator flux vector. This is the basic principle of DTC. Fig. 2 shows the block diagram of DTC.

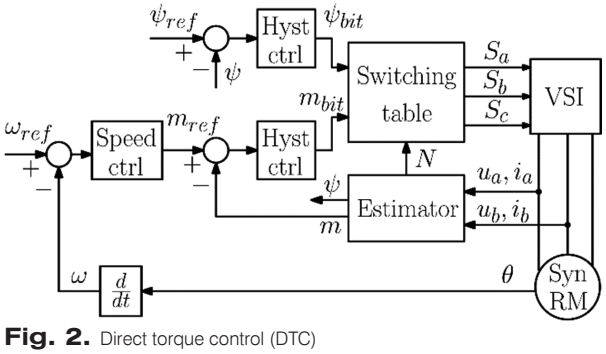

Fig. 2. Direct torque control (DTC)

According to Fig. 2, the electromagnetic torque and the amplitude of the stator flux vector are controlled by hysteresis controllers (Hyst ctrl in Fig. 2). The output of the hysteresis controllers (ψ_{bit} and m_{bit}) are input to a switching table, which uses the sector number of the stator flux vector (N in Fig. 2) as well in order to control the two-level, three-phase voltage-source inverter (VSI in Fig. 2; the switching signals are marked with S_a, S_b and S_c).

An estimator is used for the estimation of m, ψ and N. The estimator uses the measured currents and voltages in order to make the estimation. The amplitude of the stator flux vector can be estimated in the following way:

$$\psi_x = \int (v_x - Ri_x)\, dt \tag{11}$$

$$\psi_y = \int (v_y - Ri_y)\, dt \tag{12}$$

$$\psi = \sqrt{\psi_x^2 + \psi_y^2} \tag{13}$$

where v_x and v_y are the real-axis and the imaginary-axis components of the stator voltage vector in the two-phase stationary coordinate system (so-called x–y coordinate system, where the x-axis is fixed to the a-phase axis of the abc three-phase coordinate system), respectively. The definitions of i_x and i_y and ψ_x and ψ_y are similar.

The angle of the stator flux vector in the x–y coordinate system is

$$\gamma = \arctan\left(\frac{\psi_y}{\psi_x}\right) \tag{14}$$

If $330° \le \gamma$ or $\gamma < 30°$, then $N = 1$; if $30° \le \gamma < 90°$, then $N = 2$; etc. Each sector spans $\pm 30°$ around the active voltage vectors belonging to the switching states of the inverter in the x–y coordinate system (Fig. 3; the sector numbers are marked with red). This means that it is not necessary to know the exact position of the stator flux vector and is enough to determine its sector number, which means that a position determination accuracy of electrical degree of 60 is sufficient. This is a significant advantage over other torque-control algorithms. In Fig. 3, the stator flux vector resides in the fourth sector.

Table 1 shows the switching table that is used by DTC. The outputs of the torque and the flux hysteresis controllers (ψ_{bit} and m_{bit}) along with the sector number of the stator flux vector (N_1, …, N_6 in Table 1) determine the voltage vector that is to be switched on the motor terminals. The interpretation of the voltage vector numbers in Table 1 is based on Fig. 3.

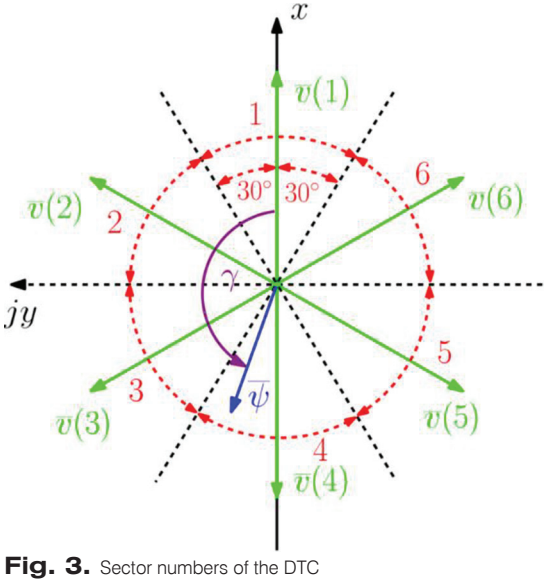

Fig. 3. Sector numbers of the DTC

Table 1. The switching table of the DTC

ψ_{bit}	m_{bit}	N_1	N_2	N_3	N_4	N_5	N_6
1	1	2	3	4	5	6	1
	0	6	1	2	3	4	5
0	1	3	4	5	6	1	2
	0	5	6	1	2	3	4

The DTC is used in the case of other motor types as well. Detailed descriptions of the DTC can be read in Buja and Kazmierkowski (2004), Grabowski et al. (2000), Juhasz et al. (2000), Malinowski et al. (2001, 2003), Orłowska-Kowalska and Dybkowski (2016), Schmidt and Veszpremi (2005), Veszpremi and Schmidt (2008), Zhang and Foo (2016) and Zhang et al. (2015).

Based on the short description given in this section, it can be concluded that the DTC has the following advantages:

– The method is simple and robust because hysteresis controllers are being used, there is no need to know the exact position of the stator flux vector and a switching table is used in order to determine the required voltage vector.
– The realisation of the method does not require any pulse-width modulator.
– The method is less parameter sensitive than other methods because the only motor parameter that is necessary for the implementation is the stator resistance.
– The method inherently supports sensorless implementations because there is no need to know the exact position of the stator flux vector; the sector number is sufficient.

These advantages altogether explain why the DTC is considered as an attractive choice for motion control applications.

4. Hysteresis Current Vector Control

Another method that can be used for controlling the electromagnetic torque of synchronous reluctance motor drives is based on Equation (7). According to Equation (7), an optimal current vector control can be achieved if the torque angle is kept on $\vartheta_p = \pm 45°$. This means that $i_d = i_q$, and the electromagnetic torque is manipulated by changing the amplitude of the stator current vector. The flux is not controlled. If this current vector control task is achieved by means of hysteresis controllers, then the method is called HCVC. In this article, the phase-current-based HCVC is analysed. The block diagram of the method is shown in Fig. 4.

According to Fig. 4, the torque reference (m_{ref}) is fed to a reference computing block (Reference compute in Fig 4), which synthesises the phase-current reference signals ($i_{a,\text{ref}}$, $i_{b,\text{ref}}$, $i_{c,\text{ref}}$). The phase currents are controlled by hysteresis controllers (Hyst ctrl in Fig. 4). Therefore, the main advantage of this method is the simplicity.

The phase-current reference signals are synthesised in the following way. Based on Equation (8), the product of the reference values for i_d and i_q is as follows:

$$i_{d,\text{ref}} i_{q,\text{ref}} = \frac{2m_{\text{ref}}}{3p\left(L_d - L_q\right)} \tag{15}$$

Owing to the fact that $i_{d,\text{ref}}$ must be equal to $i_{q,\text{ref}}$, the following algorithm is used for the computation of the reference values:

If $i_{d,\text{ref}} i_{q,\text{ref}} \geq 0$, then

$$i_{d,\text{ref}} = i_{q,\text{ref}} = \sqrt{\frac{2m_{\text{ref}}}{3p\left(L_d - L_q\right)}} \tag{16}$$

If $i_{d,\mathrm{ref}} i_{q,\mathrm{ref}} < 0$ then

$$i_{d,\mathrm{ref}} = \sqrt{(-1) * \frac{2m_{\mathrm{ref}}}{3p\left(L_d - L_q\right)}} \tag{17}$$

$$i_{q,\mathrm{ref}} = (-1) * \sqrt{(-1) * \frac{2m_{\mathrm{ref}}}{3p\left(L_d - L_q\right)}} \tag{18}$$

After these computations, $i_{d,\mathrm{ref}}$ and $i_{q,\mathrm{ref}}$ are transformed to the x–y coordinate system and then to phase quantities in order to form $i_{a,\mathrm{ref}}$, $i_{b,\mathrm{ref}}$ and $i_{c,\mathrm{ref}}$.

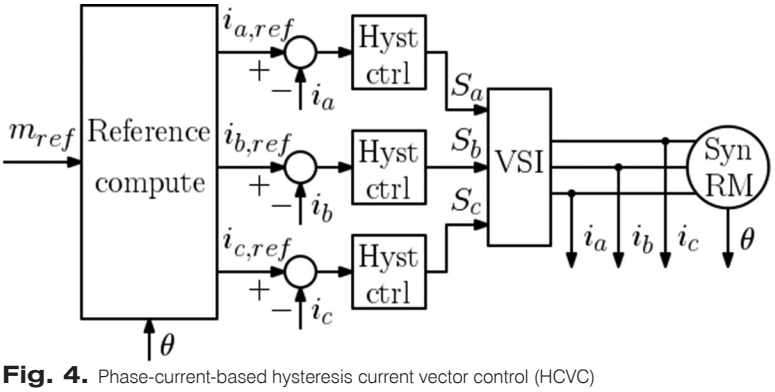

Fig. 4. Phase-current-based hysteresis current vector control (HCVC)

The HCVC methods are used in the case of other motor types as well. Detailed descriptions of these methods can be read in Mishra et al. (2016), Purohit and Dubey (2014) and Schmidt et al. (2001). Based on the short description given in this section, it can be concluded that the HCVC is a simple method for controlling the electromagnetic torque of the motor. However, the method is less robust and more parameter sensitive than the DTC because the exact position of the rotor is required in order to compute $i_{d,\mathrm{ref}}$ and $i_{q,\mathrm{ref}}$ (because the HCVC is a type of rotor position-oriented current vector control) and the computation of these signals is dependent on two motor parameters: L_d and L_q.

5. Simulation Results

Simulation was carried out for an industrial synchronous reluctance motor in the Matlab–Simulink environment, using the parameters in Table 2. Investigations were carried out for the normal operation region only (no field weakening was applied). The stator flux amplitude reference was set to its nominal value in the case of the DTC. The sample time of the torque controller varied during the investigations in order to make a comparison of the DTC and the HCVC.

Fig. 5 shows the speed reference and the actual speed for the simulated process using DTC with a 20 μs torque-control sample time. The process consists of an acceleration for up to 4000 rpm; a load–torque step of 3 Nm at 200 ms; a reversal, which is followed by the elimination of the 3 Nm load–torque at 600 ms, and finally a stopping command. Fig. 6 shows the same process for the HCVC.

Based on Figs. 5 and 6, it can be concluded that both methods are capable of realising an excellent closed-loop speed-control performance, which is essential in the case of motion control applications.

Figs. 7–12 show the torque and the amplitude of the stator flux vector and a phase current as the function of time for the DTC and the HCVC with 20 μs torque-control sample time. It can be concluded that both methods are capable of a good torque-control dynamic performance. The tracking of the torque reference is error free in the steady state in both cases. In addition, the DTC controls the amplitude of the stator flux vector in a closed-loop manner, while in the case of the HCVC, it is not controlled.

Table 2. Simulation parameters

Motor nominal speed	4000 rpm
Motor number of pole pairs	2
Motor nominal torque	3.1 Nm
Motor nominal current	6 A_{RMS}
R	1.2 Ω
L_d	43.8 mH
L_q	15.3 mH
DC-bus voltage	540 V
Total moment of inertia	3.8 kgcm^2
Speed-controller sample time	200 μs
Simulation sample time	1 μs

The main difference between the two methods is that the DTC produces visibly more torque ripples than the HCVC, which is undesirable. This difference can be noticed in the amplitude of the stator flux vector as well, but it is more visible in the current waveforms in the steady state (Figs. 11 and 12): the current waveform of the DTC is well-visibly more distorted than that of the HCVC.

The amount of torque ripples generated is an especially important aspect in the case of motion control applications. This is because an excessive amount of torque ripples can make a precise positioning significantly more difficult or even impossible. In addition, the torque ripples can cause resonances that can damage the mechanics. Based on Figs. 7 and 8, both the DTC and the HCVC are suitable for motion control synchronous reluctance motor applications: the amount of torque ripples generated is small in the case of the HCVC and tolerable in the case of the DTC. Therefore, the utilisation of the DTC is recommended in less precise applications only.

The situation gets worse if the torque-control sample time is increased up to 50 μs: the torque (Figs. 13 and 14) contains a high amount of ripples for both methods, while the current waveforms in the steady state (Figs. 15 and 16) are significantly distorted in both cases. The HCVC still produces less ripples than the DTC. Thus, it can be concluded that both the DTC and the HCVC can be used in motion control synchronous reluctance motor applications but only with a relatively high torque-control sampling frequency (approximately 50 kHz).

For example, the HCVC is suitable for more precise position control applications, conventional Computer Numerical Control (CNC) machines, etc., while the DTC is suitable for simple positioning applications, simple CNC machines (i.e. the ones that use stepper motors or brushless DC motors for positioning), etc.

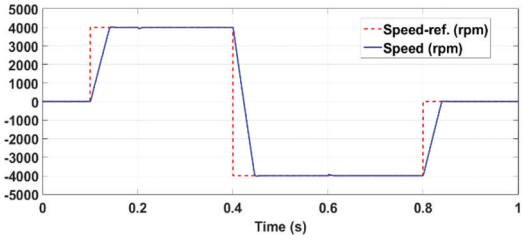

Fig. 5. The speed reference and the speed in the case of the DTC with a 20 μs torque-control sample time

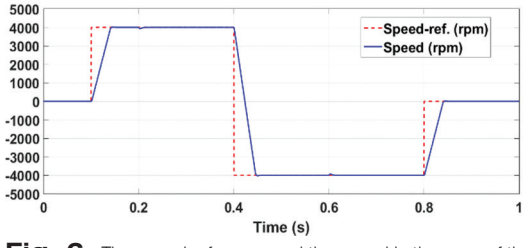

Fig. 6. The speed reference and the speed in the case of the HCVC with a 20 μs torque-control sample time

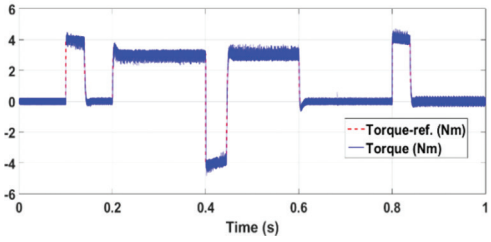

Fig. 7. The torque reference and the electromagnetic torque in the case of the DTC with a 20 μs torque-control sample time

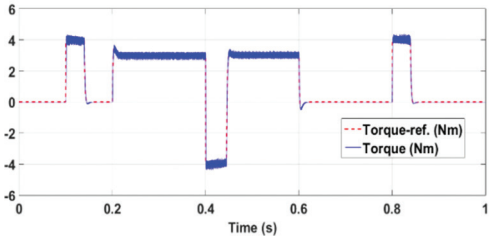

Fig. 8. The torque reference and the electromagnetic torque in the case of the HCVC with a 20 μs torque-control sample time

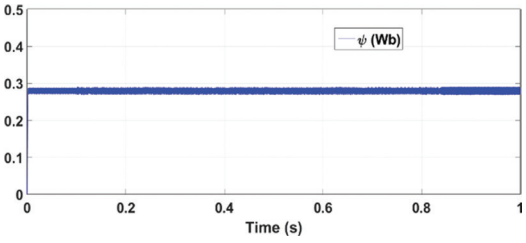

Fig. 9. The amplitude of the stator flux vector in the case of the DTC with a 20 μs torque-control sample time

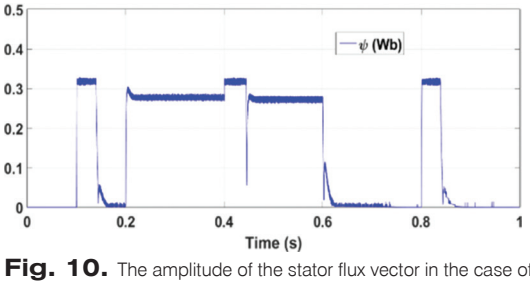

Fig. 10. The amplitude of the stator flux vector in the case of the HCVC with a 20 μs torque-control sample time

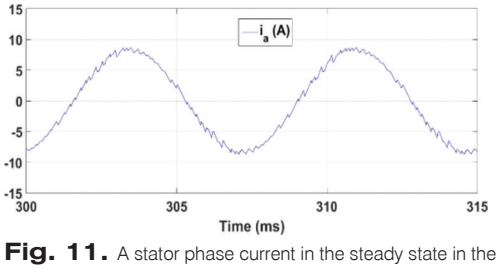

Fig. 11. A stator phase current in the steady state in the case of the DTC with a 20 μs torque-control sample time

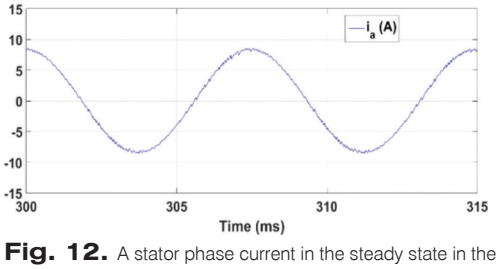

Fig. 12. A stator phase current in the steady state in the case of the HCVC with a 20 μs torque-control sample time

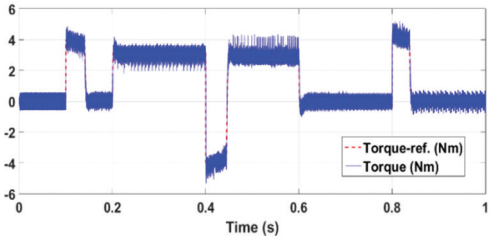

Fig. 13. The torque reference and the electromagnetic torque in the case of the DTC with a 50 μs torque-control sample time

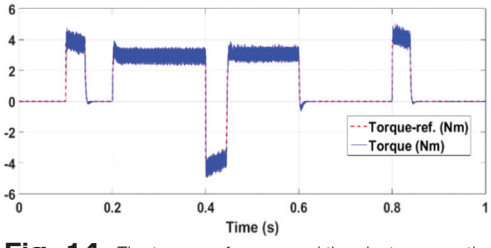

Fig. 14. The torque reference and the electromagnetic torque in the case of the HCVC with a 50 μs torque-control sample time

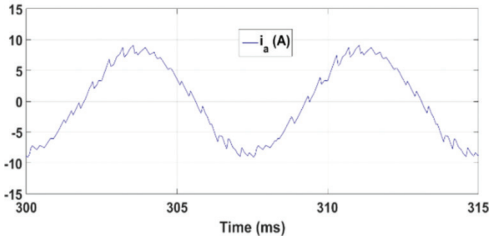

Fig. 15. A stator phase current in the steady state in the case of the DTC with a 50 μs torque-control sample time

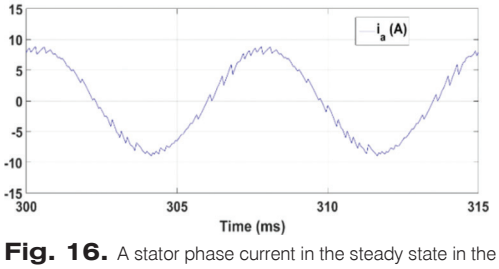

Fig. 16. A stator phase current in the steady state in the case of the HCVC with a 50 μs torque-control sample time

6. Conclusions

In this article, the DTC and the phase-current-based HCVC have been analysed for motion control synchronous reluctance motor applications. It has been concluded that both methods are capable of realising an excellent closed-loop speed-control performance.

The analysis has resulted in that the HCVC produces much less torque and current ripples than the DTC with the same torque-control sample time. In addition, it has been determined that both methods are suitable for motion control synchronous reluctance motor applications but require a relatively high torque-control sampling frequency (approximately 50 kHz). With this constraint, the DTC is recommended for less precise applications only, but the HCVC can be a candidate for applications requiring higher accuracy levels as well.

References

Antonello, R., Carraro, M., Peretti, L. and Zigliotto, M. (2016). Hierarchical Scaled-States Direct Predictive Control of Synchronous Reluctance Motor Drives. *IEEE Transactions on Industrial Electronics*, 63(8), pp. 5176–5185.

Bianchi, N., Bolognani, S., Carraro, E., Castiello, M. and Fornasiero, E. (2016). Electric Vehicle Traction Based on Synchronous Reluctance Motors. *IEEE Transactions on Industry Applications*, 52(6), pp. 4762–4769.

Buja, G. S. and Kazmierkowski, M. P. (2004). Direct Torque Control of PWM Inverter-Fed AC Motors — A Survey. *IEEE Transactions on Industrial Electronics*, 51(4), pp. 744–757.

Grabowski, P. Z., Kazmierkowski, M. P., Bose, B. K. and Blaabjerg, F. (2000). A Simple Direct-Torque Neuro-Fuzzy Control of PWM-Inverter-Fed Induction Motor Drive. *IEEE Transactions on Industrial Electronics*, 47(4), pp. 863–870.

Guagnano, A., Rizzello, G., Cupertino, F. and Naso, D. (2016). Robust Control of High-Speed Synchronous Reluctance Machines. *IEEE Transactions on Industry Applications*, 52(5), pp. 3990–4000.

Hadla, S. C. H. (2016). Active flux based finite control set model predictive control of synchronous reluctance motor drives. In: *2016 18th European Conference on Power Electronics and Applications (EPE'16 ECCE Europe)*, Karlsruhe (Germany), pp. 1–10.

Hinkkanen, M., Asad, A. A. H., Qu, Z., Tuovinen, T. and Briz, F. (2016). Current Control for Synchronous Motor Drives: Direct Discrete-Time Pole-Placement Design. *IEEE Transactions on Industry Applications*, 52(2), pp. 1530–1541.

Juhasz, G., Halasz, S. and Veszpremi, K. (2000). New aspects of a direct torque controlled induction motor drive. In: *Proceedings of IEEE International Conference on Industrial Technology 2000 (IEEE Cat. No.00TH8482)*, Goa (India), pp. 43–48.

Ma, X., Li, G., Zhu, Z., Jewell, G. W. and Green, J. (2018). Investigation on Synchronous Reluctance Machines with Different Rotor Topologies and Winding Configurations. *IET Electric Power Applications*, 12(1), pp. 45–53.

Malinowski, M., Kazmierkowski, M. P., Hansen, S., Blaabjerg, F. and Marques, G. D. (2001). Virtual-Flux-Based Direct Power Control of Three-Phase PWM Rectifiers. *IEEE Transactions on Industry Applications*, 37(4), pp. 1019–1027.

Malinowski, M., Kazmierkowski, M. P. and Trzynadlowski, A. M. (2003). A Comparative Study of Control Techniques for PWM Rectifiers in AC Adjustable Speed Drives. *IEEE Transactions on Power Electronics*, 18(6), pp. 1390–1396.

Mishra, T., Devanshu, A., Kumar, N. and Kulkarni, A. R. (2016). Comparative analysis of Hysteresis Current Control and SVPWM on Fuzzy Logic based vector controlled Induction Motor Drive. In: *2016 IEEE 1st International Conference on Power Electronics, Intelligent Control and Energy Systems (ICPEICES)*, Delhi (India), pp. 1–6.

Nardo, M. D., Calzo, G. L., Galea, M. and Gerada, C. (2018). Design Optimization of a High-Speed Synchronous Reluctance Machine. *IEEE Transactions on Industry Applications*, 54(1), pp. 233–243.

Orłowska-Kowalska, T. and Dybkowski, M. (2016). Industrial Drive Systems. Current State and Development Trends. *Power Electronics and Drives*, 36(1), pp. 5–25.

Purohit, P. and Dubey, M. (2014). Analysis and design of hysteresis current controlled multilevel inverter fed PMSM drive. In: *2014 IEEE Students' Conference on Electrical, Electronics and Computer Science*, Bhopal, pp. 1–5.

Schmidt, I. and Veszpremi, K. (2005). Application of direct controls to variable-speed wind generators. In: *2005 International Conference on Industrial Electronics and Control Applications*, Quito (Ecuador), pp. 1–6.

Staudt, S., Stock, A., Kowalski, T., Teigelkötter, J. and Lang, K. (2015). Raw data based model and high dynamic control concept for traction drives powered by synchronous reluctance machines. In: *2015 IEEE Workshop on Electrical Machines Design, Control and Diagnosis (WEMDCD)*, Torino (Italy), pp. 204–209.

Schmidt, I., Vincze, K., Veszpremi, K. and Seller, B. (2001). Adaptive Hyste-resis Current Vector Control of Synchronous Servo Drives With Different Tolerance Areas. *Periodica Polytechnica Electrical Engineering*, 45(3–4), pp. 211–222.

Vajsz, T., Számel, L. and Rácz, G. (2017). A Novel Modified DTC-SVM Method with Better Overload-Capability for Permanent Magnet Synchronous Motor Servo Drives. *Periodica Polytechnica Electrical Engineering and Computer Science*, 61(3), pp. 253–263.

Veszpremi, K. and Schmidt, I. (2008). Direct controls in voltage-source converters — Generalizations and deep study. In: *2008 13th International Power Electronics and Motion Control Conference*, Poznan (Poland), pp. 1803–1810.

Zhang, X. and Foo, G. H. B. (2016). A Robust Field-Weakening Algorithm Based on Duty Ratio Regulation for Direct Torque Controlled Synchronous Reluctance Motor. *IEEE/ASME Transactions on Mechatronics*, 21(2), pp. 765–773.

Zhang, X., Foo, G. H. B., Vilathgamuwa, D. M. and Maskell, D. L. (2015). An Improved Robust Field-Weakening Algorithm for Direct-Torque-Controlled Synchronous-Reluctance-Motor Drives. *IEEE Transactions on Industrial Electronics*, 62(5), pp. 3255–3264.